ALMA MATER STUDIORUM – UNIVERSITA' DI BOLOGNA

DIPARTIMENTO DI CESENA

Corso di laurea in
Ingegneria Elettronica per l'Energia e l'Informazione

Measurement of millimeter waves propagation through floors

Tesi di laurea in

Campi Elettromagnetici

Relatore

Prof. Ing. Vittorio degli Esposti

Correlatore

Prof. Ing. Enrico Maria Vitucci

Presentata da

Jacopo Scarponi

Anno accademico: 2022/2023

Contents

Contents 2
Table of illustrations 3
ABSTRACT 4
CHAPTER 1 Introduction 5
CHAPTER 2 Measurements equipment 6
2.1 Conical horn antennas 6
2.2 SG and SC compact 6
2.3 Power amplifier 8
CHAPTER 3 Methodological approach 10
3.1 Measurement setup 10
CHAPTER 4 Results and analysis 13
4.1 Results of the old residential building of the 17th century 18
4.2 Office area university building of 1930s 20
4.3 Hall university building of 1930s 22
4.4 Office area university building of 1980s 22
4.5 Modern university building of 2010 23
CONCLUSION 24
ACKNOWLEDGEMENTS 26
BIBLIOGRAPHY 27

Table of illustrations

Figure 1 Specifications of horn antennas used for the measurement campaign. 5
Figure 2 Portable spectrum analyser (left) and signal generator (right).....7
Figure 3 Gain of the power amplifier at 27 and 38 GHZ.....7
Figure 4 Antenna point-to-point alignment.....8
Figure 5 Measurement environment: Old residential building (first) Hall area of the 1930s (second) Office area of the 2010s (third) Office area of the 1930s (fourth) Office area of the 1980s (fifth) 9
Figure 6 Ways of having a wide set of data: Floor scanning along a 2m line (left) and antenna rotation along 3 points (right) 9
Figure 7 Floor structure of the modern university building of the 2010 10
Figure 8 Schematic representation of the propagation channel 12
Figure 9 Schematic representation of through slab penetration.....15
Figure 10 Scan 1 floor Pontecchio received power 18
Figure 11 Comparison of received power between the two measurements at 27GHz.....18
Figure 12 Comparison of received power between the two measurements at 38GHz.....18
Figure 13 (high) penetration attenuation 1 floor Pontecchio 19
Figure 14 (low) penetration attenuation 2 floor Pontecchio 19
Figure 15 Scan DEI Old building.....20
Figure 16 Comparison of received power between the two measurements at 27 GHz.....20
Figure 17 Comparison of received power between the two measurements at 38 GHz.....20
Figure 18 Penetration attenuation 1 floor DEI offices 21
Figure 19 Penetration attenuation 1 floor DEI old building corridors.....22
Figure 20 Penetration attenuation 2 floor DEI old building corridors.....22
Figure 21 Rotational measurements in 4 points at DEI new building 27 GHz.....22
Figure 22 Rotational measurements in 4 points at DEI new building 38 GHz.....22
Figure 23 Scan 1 floor DEI new building (high left).....23
Figure 24 Scan 1 floor DEI new building (high right) 23
Figure 25 Scan 1 floor DEI new building (low left).....23
Figure 26 Scan 1 floor DEI new building (low right).....23
Figure 27 Pavement basic structure 24

Table 1 Technical specifications of Spectrum Analyser.....7
Table 2 Technical specifications of Signal Generator.....8
Table 3 Electrical specification of the power amplifier.....9
Table 4 Electrical properties of different materials.....14
Table 5 Electrical properties and recap.....25

ABSTRACT

Due to constant advancements in technologies, millimeter waves are gaining more importance in the wireless communications field.
In the contemporary era of wireless communications, more and more devices are connected each year, with this number expected to increase exponentially in the following ones. To handle the increase in the number of end users, research is going on towards next generation cellular networks such as 5G, 6G and beyond.
When considering mm-wave propagation, indoor propagation becomes of particular interest since even the smallest objects would produce significant attenuation at those high frequencies [2].
Indoor structures, especially in modern construction techniques, are known to heavily hinder the signal propagation indoors. One aspect of indoor propagation that is very useful in interference management or coverage prediction problems, is the propagation through the floors.
In this work, we conduct several measurements related to through floor attenuation in different typical Southern European buildings. Given the gap in the existing literature, this work aims at giving some representative values of attenuation each floor suffers from, according to the construction type and year of each considered building.
The thesis begins with an introduction to the millimeter wave frequency range and a description of all the measurement equipment that we used.
Then, measurement results at each location will be described for all the considered points. The conclusion contains a summary of the thesis with a table that shows the electrical properties of different floor slabs.

CHAPTER 1 Introduction

The World Radiocommunication Conference 2015 (WRC-15) identified several frequency bands between 24 and 86 GHz as candidate frequencies for future cellular networks.

One important issue of mm-wave propagation is the higher path loss, A radio channel is defined as the part of air communication link between the transmitting and receiving antenna. Under ideal conditions, a radio channel would be under the so-called free space propagation, meaning that there is no interference or disturbance to the channel from external sources. This means that the free space path loss will be the only variable affecting the received power. However, in real world scenarios, free space is rarely occurred especially in open big outdoor environments. In real world scenarios, fading or shadowing are almost always present, causing a decrease in the received power with respect to the one suffering from free space path loss only. As such, channel becomes unpredictable and the major limits towards achieving high data rates, low latency, and good quality of service. The use of high-gain antenna arrays is therefore one of the ways in which we can mitigate this problem. Other important issues are gaseous and rain attenuation for longer range links and higher shadowing due to lower diffraction and penetration in case of line-of-sight (LOS) blockage from obstacles [1].

Given the link-distance limitations, the foreseen application scenarios of mm-wave transmission are limited to outdoor backhauling and front-hauling links and outdoor or indoor access links in LOS or quasi-LOS conditions. In the case of outdoor small cell links, it is, in principle, necessary to consider the additional attenuation due to gases in the lower atmosphere and rain. In the frequency range up to 100 GHz, two absorption peaks occur in standard atmosphere. The larger one is due to oxygen at 60 GHz and corresponds to 15 dB/km. Therefore, gas attenuation should not represent a major concern for future mm-wave indoor and small-cell applications. Similar considerations hold true for rain effects, with a maximum attenuation of about 30 dB/km for very heavy (100 mm/h) rainfall [1]. As most of the data traffic is now confined indoors, ensuring seamless radio coverage is of paramount importance, whether from outdoor or indoor base stations or access points. Consequently, propagation mechanisms in and around buildings become crucial, particularly for millimeter-wave frequencies. One such mechanism governing indoor propagation is the transmission between different floors of a building. Unfortunately, floor penetration attenuation significantly compromises indoor coverage, especially at millimeter-wave frequencies. This substantial attenuation results in a dual outcome: it is undesirable when the primary goal is uninterrupted coverage, yet it can suppress interference, which is desirable in many applications.

However, it is important to highlight the insufficient data available in the literature regarding the specific challenges posed by these frequencies, with existing studies predominantly focused on lower frequency bands.

Considering this literature gap, this study aims to contribute to a deeper understanding of propagation mechanisms, particularly those related to the transmission between different floors of a building, providing an insight on their penetration loss that will have an impact in important aspects of mm-wave propagation characterization, for future 5G systems and applications.

CHAPTER 2 Measurements equipment

2.1 Conical horn antennas

In the following chapter, we provide a description of measurement equipment used during measurement campaigns. The antennas that we used for this scope where SAF Tehnika antennas. Since the measurements need to be point-to-point, directional antennas are needed both at the transmitter and receiver side. The antennas used were compact, lightweight, and reliable conical horn antenna. Furthermore, a SAF Signal generator was used to feed the transmitting horn antenna and a portable SAF spectrum analyser was connected to the receiving horn antenna.

The Half power beamwidth (HPBW) is a parameter that indicates the amplitude of the angle at which the antenna radiates half of its maximum power. The E-plane and H-plane are related to this parameter. Figure 1 shows that if the frequency rises than the beamwidth of the antenna is decreasing, making the antenna more directive.

Electrical and mechanical specifications

P/N	J0AA2640HG03
Operating frequency, GHz	26.500-40.500
Gain (typical), dBi	20.5-21.5
HPBW *E-plane:* ~14° @ 26.5 GHz ~13.5° @ 28 GHz ~13° @ 30 GHz ~12.5° @ 32 GHz ~12° @ 36 GHz ~11.5° @ 38 GHz ~11° @ 40 GHz	*H-plane:* ~17.5° @ 26.5 GHz ~16.5° @ 28 GHz ~15.5° @ 30 GHz ~15° @ 32 GHz ~13.5° @ 36 GHz ~13° @ 38 GHz ~12.5° @ 40 GHz
Dimensions, mm/inch	120 x 86 x 60/4.7 x 3.4 x 2.4
Net weight, kg/lb	0.4
Flange (connector)	2.92 mm (K)
Matching Spectrum Compact unit	J0SSAP14

Figure 1 : Specifications of horn antennas used for the measurement campaign.

2.2 SG and SC compact

The Spectrum Compact is a radio wave measurement and analysis tool used to monitor and analyse the spectrum of radio frequencies. Such instruments are commonly used in the telecommunications industry, wireless networks, radio communication, and other applications where monitoring frequency bands and identifying interference or signal issues are important. Spectrum Compact is an ultra-light and easy to use measurement solution. It operates in a frequency range of 2 - 40 GHz and is a battery-powered device. Both SG and SC compact must be used with the corresponding radio frequency (RF) cable. In this case, as we utilized the 26.500 to 40.500 GHz conical horn antennas, we employed a cable tailored to this frequency range.

The difference between the two spectrum is that the SC is the receiver, and the SG is the generator. Both antennas were mounted on a tripod specifically designed for measurement campaigns to ensure stability during our measurements.

The output resistance of the SG (transmitter) is the same of the input resistance of the SC (receiver). This can be explained looking at the theory about the matching of the characteristic impedance of a trace. We know in fact that in many applications, especially those involving RF (radio frequency) signals or high-frequency electrical signals, it's important for the output impedance of the transmitter to match the input impedance of the receiver to optimize transmission efficiency and minimize signal reflections. This concept is known as impedance matching. The output impedance of the transmitter and the input impedance of the receiver should either be the same or chosen to be compatible with each other. It's common to use 50 ohms as the characteristic impedance in RF applications. Therefore, an RF transmitter with a 50-ohm output is typically connected to an RF receiver with a 50-ohm input. Impedance matching helps minimize signal reflections between the transmitter and the receiver, which can cause power loss and signal distortion.

Figure 2: Portable spectrum analyser (left) and signal generator (right)

1.2 Technical specification

P/N	J0SSAG11	J0SSAG12	J0SSAG13	J0SSAG14
Frequency bands	6/7/8/10/11 GHz	10/11/13/15/17 GHz	17/18/23/24 GHz	24/26/30/32/38 GHz
Frequency range	5.925-12.000 GHz	10.000–18.000 GHz	17.000–24.300 GHz	24.000-40.000 GHz
Output power range	-3…+13 dBm	-3…+11 dBm	-3…+10 dBm	-3…+5 dBm
Adjustable frequency step	1 MHz			
Adjustable power step	1 dBm			
Signal form	Continuous wave			
Guaranteed accuracy	+/- 1 dBm			
Interface	mini USB 2.0 (1.1)			
Operating temperature	-15°C to +40°C / 5°F to 104°F			
Battery	LiPo 2200 mAh (3.7V)			
Battery life	up to 4h			up to 3h
Output	50 ohm SMA (f)			50 ohm 2.92mm (f)
Dimensions	128 x 81 x 24 mm / 5.04 x 3.2 x 0.94 in			130 x 81 x 28 mm / 5.11 x 3.2 x 1.1 in
Weight	0.3 kg / 10.6 oz			0.4 kg / 14.11 oz

Table 1: Technical specifications of Spectrum analyser

Technical Specifications

Spectrum Compact

P/N	J0SSAP11	J0SSAP12	J0SSAP13	J0SSAP14
Frequency bands	6/7/8/10/11 GHz	10/11/13/15/17 GHz	17/18/23/24 GHz	24/26/30/32/38
Frequency range	5.925 - 12.000 GHz	10.000 - 18.000 GHz	17.000 - 24.300 GHz	24.000-40.000 GHz
Input power range	-105 dBm to -40 dBm			-100 dBm to -40 dBm
Max input power	0 dBm			0 dBm
RBW (Resolution bandwidth)	1 MHz			1 MHz
Span	100 MHz to full bandwidth			100 MHz to full bandwidth
Sweep speed	0.5s @ 100 MHz Span			0.5s @ 100 MHz Span
Guaranteed accuracy	+/- 3 dB			+/- 3 dB
Input	50 ohm SMA (f)			50 ohm 2.92 mm (f)
Interface	mini USB 2.0 (1.1)			mini USB 2.0 (1.1)
LED indication	when charging			when charging
Battery	2380 mAh Polymer Lithium-ion			2 x 2380 mAh Polymer Lithium-ion
Battery life	up to 4h			up to 3h
Operating temperature	-5°C to +40°C / 23°F to 104°F			-5°C to +40°C / 23°F to 104°F
Dimensions	128 x 81 x 24 mm / 5.04 x 3.2 x 0.94 in			130x81 x 28 mm/ 5.11 x 3.2 x 1.1 in
Weight	0.3 kg / 10.6 oz			0.4 kg/ 14.11 oz

* coaxial cable or frequency specific SAF adapter kit will be required

Table 2: Technical specifications of Signal generator

2.3 Power amplifier

We used the Model SBP-2734033020-KFKF-S1 which has a small typical signal gain of 30 dB and a nominal P1dB of +20 dBm across the frequency range of 26.5 to 40 GHz. The P1dB of +20dBm means that the signal change of 1 dB from the linear form, if we use an input power over +20dBm. In telecommunications, return loss is the attenuation of the signal that is reflected due to one or more discontinuities in a transmission line. Specifically, a discontinuity can be caused by:

- A difference in impedance between the line and its resistive termination load.
- A difference in impedance between the line and any devices inserted along its path.
- Damage to the line.

Return loss is defined as the following ratio in decibels (dB):

$$RL(dB) = 10 * log_{10} \frac{P_i}{P_\rho} \tag{2.3.1}$$

So, the higher the return loss the higher the performances are, due to a better conjunction between the different impedances. In the amplifier we can see two electrical specification that represent the return loss and they are “input return loss” and “output return loss”. A value of 7dB is acceptable in lots of devices. “P_{1dB}” is a critical parameter in the specifications of electronic devices, particularly amplifiers. It indicates the maximum input power level at which the output of a device, such as an amplifier, experiences a 1 dB compression of the signal compared to its ideal linear response. In simpler terms, when the input signal power exceeds the P1dB, the device's output begins to behave in a non-linear manner, which means that the amplifier no longer increases the input signal proportionally. Instead, its response starts to "compress" the signal, leading to distortions and changes in the waveform. The maximum Pin that can be used in fact is way under this upper limit. In the setup of measurement

campaigns, the amplifier is consistently cooled by a fan to prevent excessive heating and subsequent malfunctions.

Electrical Specifications:

Parameter	Minimum	Typical	Maximum
Frequency	26.5 GHz		40.0 GHz
Gain		30 dB	
P_{1dB}		+20 dBm	
P_{in}			+8 dBm
Input Return Loss		7 dB	
Output Return Loss		7 dB	
DC Voltage	+6 V_{DC}	+8 V_{DC}	+15 V_{DC}
DC Supply Current		280 mA	
Specification Temperature		+25 ˚C	
Case Temperature	0 ˚C		+50 ˚C

Table 3: Electrical specifications of the power amplifier

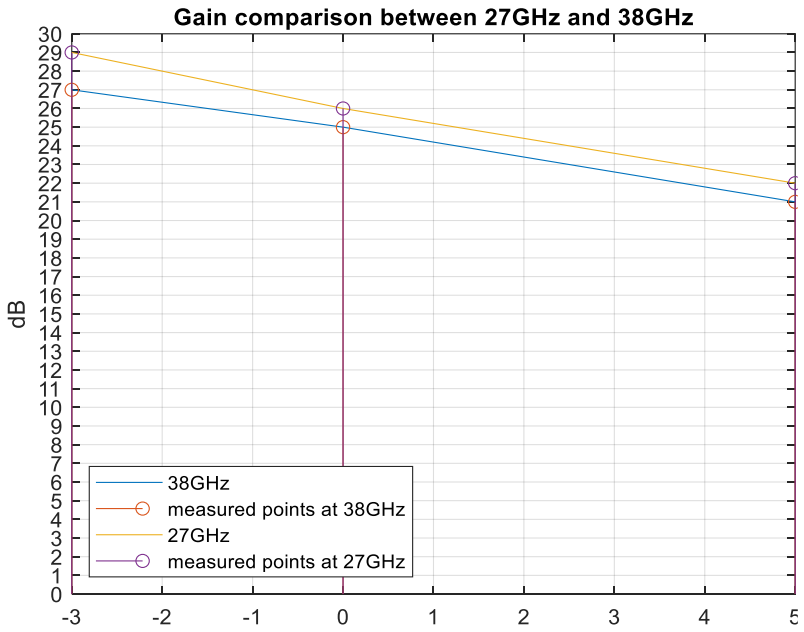

Figure 3: Gain of the power amplifier at 27 and 38 GHZ

We focused more on the power amplifier because we noticed that increasing or decreasing the input power, the gain of the amplifier and therefore the total gain, were changing. This is because the amplifier has a fixed output power, so increasing the input power the gain decreases to maintain the same output power. In this plot is showed the difference in Gain between the two frequencies at different input powers of the amplifier. To highlight this change of behaviour we made different measurements, changing the frequency and the input power. We made 6 measurements, each one took more than one attempt to be definitive, to ensure the fidelity of the result. Each power input has two different frequencies, 27GHz and 38GHz. The plot shows an almost linear variation of the amplifier gain in each frequency with respect to input power.

CHAPTER 3 Methodological approach

In the following chapter, a detailed description of the measurement environment is performed. In order to have a wide set of data, we carry measurement campaigns in four different types of buildings in Italy, each constructed in a different period with different construction techniques and materials. The ability of radio waves to penetrate buildings depends on several factors, including the frequency of the waves, the materials of the building, and the thickness and density of the walls. Generally, lower frequency radio waves, such as those used by AM radio stations, are better at penetrating buildings compared to higher frequency waves used by FM radio or cellular networks. This is because lower frequency waves have longer wavelengths, which can more easily bend around obstacles. Materials like concrete and brick can hinder the penetration of radio waves to some extent, as they are denser and absorb or reflect some of the energy. However, these materials do not completely block radio waves, and they still allow a significant portion of the signal to pass through. Buildings with metal or metallic coatings, on the other hand, can significantly reduce or block radio waves due to their high conductivity. In some cases, radio waves can also penetrate buildings through windows and other openings. Glass is transparent to radio waves, allowing the signal to pass through without significant attenuation. Overall, while buildings may slightly weaken or attenuate radio waves, they do not completely prevent their penetration. This is why radio signals can still be received indoors, although their strength may be reduced compared to outdoor environments.

3.1 Measurement setup

In the following a brief description of the measurement setup is done. Since antenna stability is of paramount importance in this point-to-point measurement setup, we make use of the tripods that are made especially for the measurement campaigns. Both horn antennas are put on tripods that are then aligned vertically in different floor as can be seen from the Figure 4 : Antenna point-to-point alignment It is important to ensure the correct alignment of the transmitter and receiver antennas: as such floor with a certain level of symmetry were chosen as measurement environments.

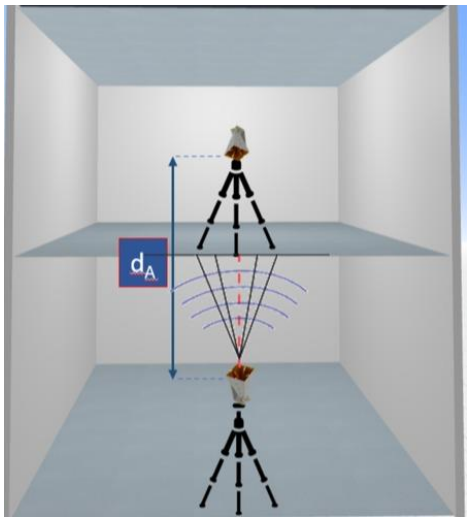

Figure 4 : Antenna point-to-point alignment

A median value of 16 samples was taken directly at the receiver side to filter out the random fluctuations in time. For verifying the measurement repeatability and having higher accuracy, different values were read at the same point apart from the 16-sample median that was already pre-set at the receiver. The

distance between the 2 antennas, noted as d_A in the figure 4, is given in the table at page 29 (Conclusion). Having a wide set of propagation data is crucial for verifying the measurements' reliability. As such, transmitter and receiver are moved to different positions inside the same room/hall where possible, or antennas are rotated by 120° due to a rotor installed in both tripods (see Figure 6). This way an accurate insight of the losses when signal passes through the floors is achieved. Since our aim is to investigate the through-floor propagation in different building types, five representative types of buildings were identified and considered for this measurement campaign as seen from the figure 5

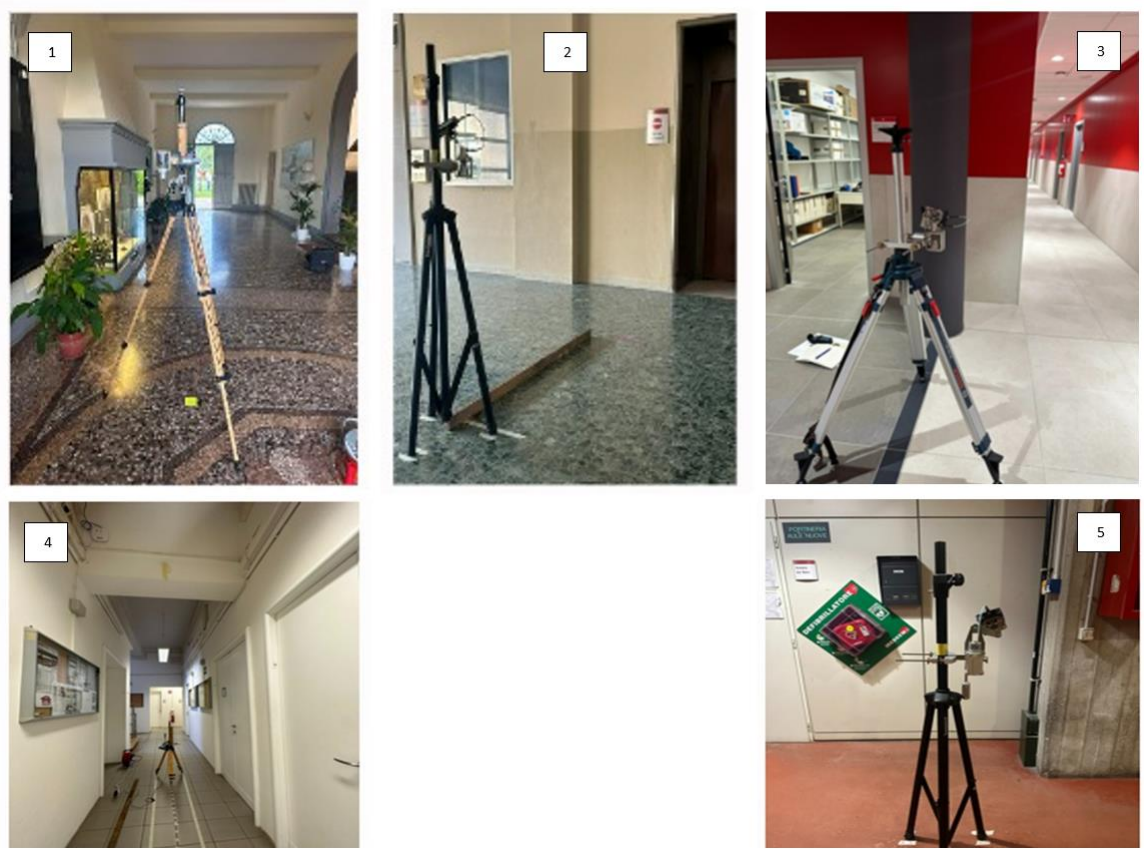

Figure 5: Measurement environment: Old residential building (first) Hall area of the 1930s (second) Office area of the 2010s (third) Office area of the 1930s (fourth) Office area of the 1980s (fifth)

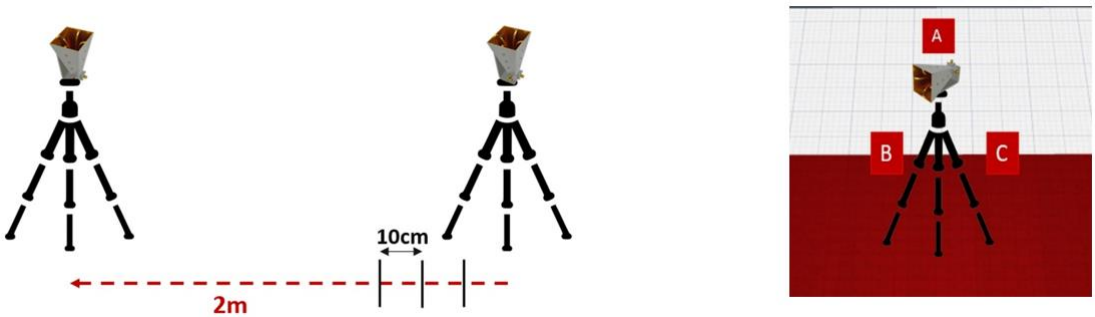

Figure 6: Ways of having a wide set of data: Floor scanning along a 2m line (left) and antenna rotation along 3 points (right)

1. Old residential building of the 17th century

The first building under consideration is an old residential building constructed in 17-th century. Its floor is made from wooden structures. Due to potential unevenness in the floor structure of old buildings, measurements of losses through the floor are repeated 21 times by changing simultaneously with 10 cm along a straight predefined line. This method allows for a 2-meter scan of the floor moving forwards and then backwards along a line as seen from the left of the Figure 6. Moreover, as wooden structures theoretically exhibit lower losses compared to reinforced concrete found in modern buildings, measurements of propagation through two floors are performed to assess if it is possible for the signal to propagate through two floors. This involved placing the transmitter on the first floor and the receiver on the third floor. Here, due to the presence of furniture preventing a linear movement of the receiver on the third floor, thus preventing a comprehensive scan, six different measurements have been taken by rotating both the antennas with 120°, keeping the same fixed position of the tripods, as shown in position A, B, C in right of the Figure 6. This process is repeated twice for each rotation position. The antenna has been placed below, was at circa 20 meters from the entrance, few meters over the beginning of the stairs and the other antenna perpendicular to the first one.

2. Office area university building of the 1930s

The second scenario is the University office area that was built around 1930 and has floors made of reinforced concrete (second case in Figure 5). Floor thickness in this case is 30 cm. In this building, as in the previous old residential building, measured points were taken along a straight line, for a total of 16 locations with 30 cm spacing between each-other, forward, and backward on the same points for double check.

3. Hall university building of the 1930s

The third measurement environment is the hall of the University building (third case in Figure 5) built around the year 1930, that has floors made of reinforced concrete. Here, apart from the floor thickness (28.5 cm), a 40 cm false ceiling is present, with several cables, ducts, and pipes. In this scenario, a 2m horizontal scan is performed, moving simultaneously both the transmitter and receiver with a 10cm step on a straight line, as done in the old residential building. An attempt to measures losses through two floors was made also in this scenario, but it resulted that, as expected given the reinforced concrete structures, the received signal fell below noise floor.

4. Office area university building of the 1980s

In the most recent section of the building, we paired the previous method, used in DEI corridor, with a displacement of the antennas in for different direction. Each direction taken were 90 degrees rotated in respect to the previous displacement, to form a square. In this way we have in the vertices of the square three measurements each at 120 angle degrees to the other

5. Modern university building of the 2010

The Cesena location was constructed even later, well into the 21st century, and this resulted in a flooring structure that didn't provide us with useful received power values at any point.

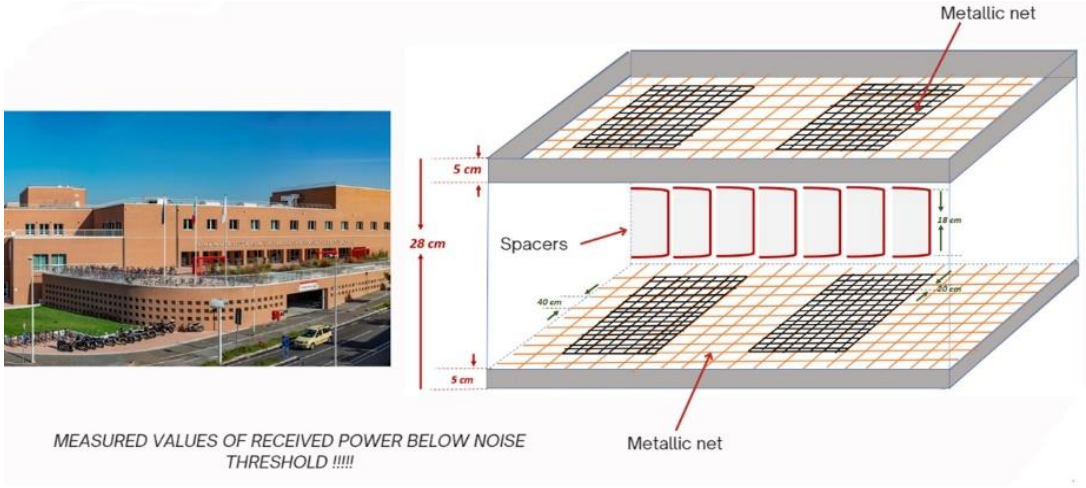

Figure 7: Floor structure of the modern university building of the 2010

CHAPTER 4 Results and analysis

In this chapter, an analysis of the measurements conducted is presented. Our main interest is the received power value in the case where a floor is present between the transmitter and the receiver. Furthermore, the mean attenuation and the standard deviation of the floor penetration losses are two figures of great interest in the post processing of the data. Through a simple MATLAB script, we obtain the aforementioned figures.

.

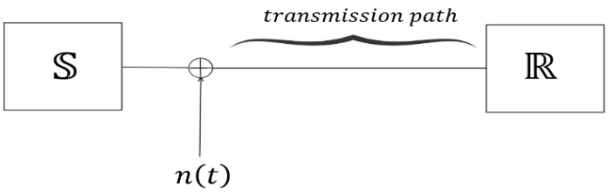

Figure 8: Schematic representation of the propagation channel

Our measurement system is composed of two blocks: a source and a receiver, respectively S and R as depicted in Figure 8: Schematic representation of the propagation channel.

The source is the SAF spectrum generator who creates an internal signal than propagates in a predefined direction, being the horn antenna highly directive. The receiver is able to receive the transmitted signal, with a certain loss that depends on the propagation conditions. The external noise is also to be considered, which is added into the system at the beginning. The noise is an important thing to consider because it tells us weather the measurements done are valid or not: if received signal falls below the noise level, that measurement value is to be discarded.

For instance, in the most modern university building of the 2010, as mentioned before, we obtained values that were below the noise threshold. In this case, we could not extract any information from the measurements since we could not distinguish the signal from the noise. The transmission path is the path between the transmitter and receiver where the signal is transmitted, including all the things that could be in the middle. Consequently, attenuation as a function of the distance between the transmitter and receiver ends is easily calculated. In this work the transmission path is always composed by air for most of the length and then by compose materials that constitute the floor slab when the signal starts to propagate within the material. The transmission loss due to the air is calculated by the means of the Friis equation:

$$P_R = P_T G_T G_R \left(\frac{\lambda}{4\pi R}\right)^2 \tag{4.1}$$

That can also be written in dB:

$$P_R dB = P_T dB + G_T dB + G_R dB + 20log\left(\frac{\lambda}{4\pi R}\right) \tag{4.2}$$

Where P_T is the transmitted power in dB, G_T and G_R are the gains of the transmit and receiving antenna respectively and R is the distance between the two antenna ends. Wavelength is denoted as λ .Firstly, we calculate the free space path loss, and we get the final value of the power received theoretically. We substitute in equation 4.2 the appropriate values of $P_T = 0\ dB$, $G_T = 21\ dB$, G_R We subtract from the Friis equation the value measured and we get a value that is called supplementary attenuation. We have also calculated using a bit of assumption in the matter of the material composition, the permittivity and conductivity of the floor slab.

This is the table we used as reference.

Material class	Relative permittivity		Conductivity		Frequency range
	a	*b*	*c*	*d*	GHz
Concrete	5.31	0	0.0326	0.8095	1-100
Brick	3.75	0	0.038	0	1-10
Plasterboard	2.94	0	0.0116	0.7076	1-100
Wood	1.99	0	0.0047	1.0718	0.001-100
Glass	6.27	0	0.0043	1.1925	0.1-100
Ceiling board	1.50	0	0.0005	1.1634	1-100
Chipboard	2.58	0	0.0217	0.7800	1-100
Floorboard	3.66	0	0.0044	1.3515	50-100
Metal	1	0	10^7	0	1-100
Very dry ground	3	0	0.00015	2.52	1-10 only
Medium dry ground	15	−0.1	0.035	1.63	1-10 only
Wet ground	30	−0.4	0.15	1.30	1-10 only

Table 4 electrical properties of different materials

According to the composition of the slab, we calculated an approximated conductivity (thanks to table 4) and than calculated the permittivity. Now we will see how we managed to do it and how the

loss through materials works. The antennas were perpendicular so we assumed that there was no multiple reflection inside the slab, if there was a slope between the two antennas instead it would be not as shown in the image below but with more reflection. The image below is only theoretical, it doesn't show exactly the way we operated (it is not perpendicular). There is a reflection anyway in both the first external part of the slab and the second internal part. In the equation we calculated the

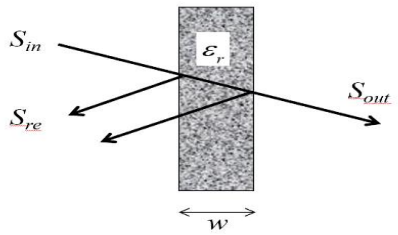

Figure 9: Schematic representation of through slab penetration

reflection coefficient, that due to a normal incidence is simplified as we see in: $\frac{1-\sqrt{\varepsilon_r}}{1+\sqrt{\varepsilon_r}}$.

$$\frac{\cos(\theta_i) - \sqrt{\left(\frac{n_2}{n_1}\right)^2 - sin^2_{\theta_i}}}{\cos(\theta_i) + \sqrt{\left(\frac{n_2}{n_1}\right)^2 - sin^2_{\theta_i}}} = \frac{1-\sqrt{\varepsilon_r}}{1+\sqrt{\varepsilon_r}} \quad , \theta_i = 0 \tag{4.3}$$

Than operating with the pointing vector, that is representing the power, we get a relation between two equations.

$$\frac{S_{re}}{S_{in}} = \frac{\frac{|E_{re}|^2}{2\eta}}{\frac{|E_{in}|^2}{2\eta}} = \frac{|E_{re}|^2}{|E_{in}|^2} = |\Gamma|^2 \tag{4.4}$$

We have to find at the end the power loss, so the second equation will be very useful.

In electromagnetism, the absolute permittivity, often simply called permittivity and denoted by the Greek letter ε (epsilon), is a measure of the electric polarizability of a dielectric. A material with high permittivity polarizes more in response to an applied electric field than a material with low permittivity, thereby storing more energy in the material. In electrostatics, the permittivity plays an important role in determining the capacitance of a capacitor.

In a mean with losses, the propagation constant can be written as:

$$k = w\sqrt{\mu_0 \varepsilon_c} = \sqrt{\mu_0 \varepsilon_0 \varepsilon_r} \tag{4.5}$$

Where ε_c is the complex permittivity. As opposed to the response of a vacuum, the response of normal materials to external fields generally depends on the frequency of the field. This frequency dependence reflects the fact that a material's polarization does not change instantaneously when an electric field is applied. The response must always be causal (arising after the applied field), which can be represented by a phase difference. For this reason, permittivity is often treated as a complex function of the (angular) frequency ω of the applied field:

$$\varepsilon \rightarrow \varepsilon(w) \tag{4.6}$$

We can write the relative complex permittivity as below:

$$\varepsilon_r = \varepsilon'_r - j\varepsilon''_r = \frac{\varepsilon}{\varepsilon_0} - \frac{\sigma}{w\varepsilon_0} \tag{4.7}$$

-ε'_r represents the real part of complex permittivity and is also referred to as "dielectric permittivity." This component describes a material's ability to store electrical energy when subjected to an oscillating electric field. In other words, epsilon' indicates the conservative part of the material's response to the oscillating electric field.

-ε''_r represents the imaginary part of complex permittivity and is also known as "conductive permittivity" or "dielectric loss." This component describes a material's ability to dissipate energy under the influence of an oscillating electric field, typically due to conductivity effects or energy losses.

- σ represents the conductivity, is the measure of the ease at which an electric charge or heat can pass through a material. A conductor is a material which gives very little resistance to the flow of an electric current or thermal energy.

We can see that the imaginary part of the permittivity is proportional to sigma, which is calculated with this formula, using the table 1 as reference, as already mentioned.

$$\sigma = (c * f)^d \tag{4.8}$$

A plane wave who propagates itself into a mean has this equation:

$$E = E_0 e^{-jkr} = E_0 e^{-(\alpha + j\beta)r} \; where \; jk = \alpha + j\beta$$

Where:

$$k = w\sqrt{\mu_0 \varepsilon_0 \varepsilon_r} = w\sqrt{\mu_0 \varepsilon_0} * \sqrt{\varepsilon'_r - j\varepsilon''_r} = \frac{w}{c}\sqrt{\varepsilon'_r} * \sqrt{1 - \frac{j\varepsilon''_r}{\varepsilon'_r}} \approx \frac{w}{c}\sqrt{\varepsilon'_r}\left(1 - \frac{j\varepsilon''_r}{2\varepsilon'_r}\right) \tag{4.9}$$

$$jk = \alpha + j\beta \approx \frac{w}{c}\sqrt{\varepsilon'_r}\left(\frac{\varepsilon''_r}{2\varepsilon'_r} + j\right) \rightarrow \begin{cases} \alpha \approx \dfrac{w}{c}\sqrt{\varepsilon'_r}\left(\dfrac{\varepsilon''_r}{2\varepsilon'_r}\right) = \dfrac{\pi}{\lambda} * \dfrac{\varepsilon''_r}{\sqrt{\varepsilon'_r}} = \dfrac{\sigma}{2\varepsilon_0 c\sqrt{\varepsilon'_r}} \\ \beta \approx \dfrac{w}{c}\sqrt{\varepsilon'_r} \end{cases} \tag{4.10}$$

$$|E(r)| = |E(0)| * e^{-\alpha r} \tag{4.11}$$

$$S(r) = S(0) * e^{-2\alpha r} \tag{4.12}$$

After finding how to express k we can find out the expressions of alpha and beta.

-Alpha (α) represents the attenuation vector of the wave. It indicates how quickly the amplitude of the wave decreases as it propagates through the medium due to losses or energy absorption. Alpha is a positive real quantity or zero in non-dissipative materials.

-Beta (β) is the phase vector We have then some expressions for the behaviour of the pointing vector and the electric field along the distance.

Now having all these formula's we make some further steps. The reflection coefficient for the air-medium interface is given by:

$$\Gamma_{0m} = \frac{1 - \sqrt{\varepsilon_r}}{1 + \sqrt{\varepsilon_r}} \tag{4.13}$$

The reflection coefficient for the second interface, medium to air is:

$$\Gamma_{m0} = \frac{\sqrt{\varepsilon_r} - 1}{1 + \sqrt{\varepsilon_r}} = -\Gamma_{0m} \tag{4.14}$$

If we now consider the first interface, we will have:

$$\frac{S_{refl1}}{S_{inc1}} = \frac{\left|E_{refl1}\right|^2}{|E_{inc1}|^2} = |\Gamma_{0m}|^2 \tag{4.15}$$

For the conservation of power fluxes, we have:

$$S_{inc1} = S_{refl1} + S_{trasm1} \rightarrow 1 = \frac{S_{refl1}}{S_{inc1}} + \frac{S_{trasm1}}{S_{inc1}} = |\Gamma_{0m}|^2 + \frac{S_{trasm1}}{S_{inc1}} \tag{4.16}$$

$$\frac{S_{trasm1}}{S_{inc1}} = 1 - |\Gamma_{0m}|^2 \tag{4.17}$$

Now, the power density transmitted to the first interface propagates through the medium with losses and arrives at the second interface as the incident power, S_{inc2}.

$$\frac{S_{refl2}}{S_{inc2}} = |\Gamma_{m0}|^2 = |\Gamma_{0m}|^2 = |\Gamma|^2 \tag{4.18}$$

$$\frac{S_{transm2}}{S_{inc2}} = \frac{S_{transm2}}{S_{transm1} e^{-2\alpha w}} = \frac{S_{transm2}}{S_{inc2}(1 - |\Gamma|^2) e^{-2\alpha w}} = 1 - |\Gamma|^2 \tag{4.19}$$

Therefore:

Through this method we eventually calculated the permittivity and conductivity of the floor slabs.

$$\frac{S_{transm2}}{S_{inc1}} = \frac{S_{out}}{S_{in}} = (1 - |\Gamma|^2)^2 e^{-2\alpha w} \rightarrow L_t = \frac{S_{in}}{S_{out}} = \frac{e^{2\alpha w}}{(1 - |\Gamma|^2)^2} \tag{4.20}$$

[4].

We simulated this method via MATLAB, here is the script:

```
% calculates normal incidence transmission loss for a slab of known
% material using simplified Bertoni's formula
freq=38.00e9;
lambda=3e8/freq;
epsr1=6;  %sample value
sigma=1;  %sample value
thick=0.40;
eps0=8.854e-12;
epsr2=sigma/(2*pi*freq*eps0);
epsr=epsr1-1i*epsr2;
abs_gamma=abs((1-sqrt(epsr))/(1+sqrt(epsr)));
alpha=sigma/(2*eps0*3e8*sqrt(epsr1));
loss=exp(2*alpha*thick)/((1-abs_gamma^2)^2);
dB_loss=10*log10(loss)
```

By comparing the loss in dB with the value we obtained from the measures and choosing epsr1 depending on which floor slab have we operated, we get hold of the permittivity and conductivity.

4.1 Results of the old residential building of the 17th century

As it can be seen from the figure … the received power for the scanning length between 0 and 2 meters and backwards is shown. The distance between the transmitter and the receiver is 4.2 and 7.6 meters respectively.

The fluctuations that appear as we move simultaneously the transmitter and receiver from one point to another can be due to the inhomogeneity of the floor slab, composed by different materials that behave differently with each frequency.

Another thing to discuss is the mean error, to know the inaccuracy of the measure. We compared for each point, the difference in power received among the coming to and the coming back.

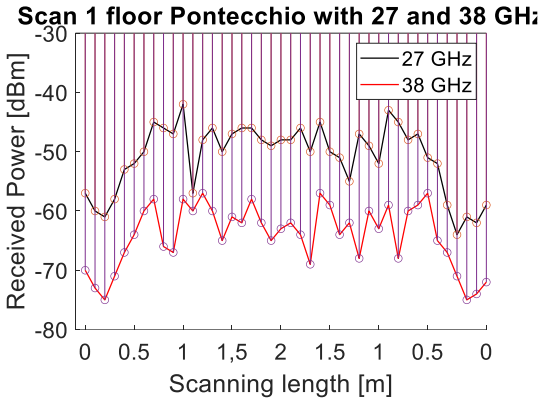

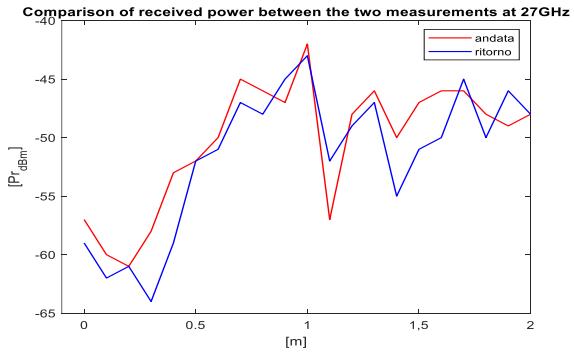

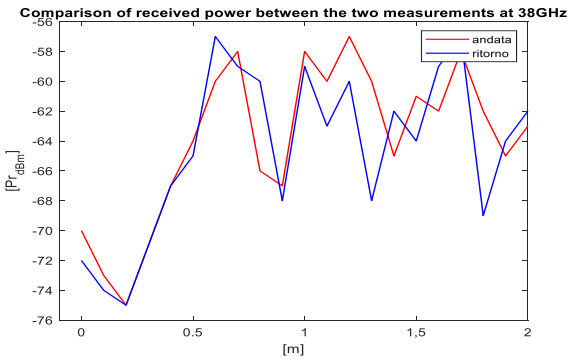

Figure 10 Scan 1 floor Pontecchio received power
Figure 11 Comparison of received power between the two measurements at 27GHz
Figure 12 Comparison of received power between the two measurements at 38GHz

Cause of this, we were able to determine the mean error of the measure, that is for 27GHz 2.3810 dB and for 38GHz 2.333 dB. We also calculated the standard deviation. We had a value of SD for 27GHz of 5.7210 and for 38GHz of 5.2894. The standard deviation is a measure of the dispersion or variability of data within a dataset. It represents how much data points deviate, on average, from the mean value. The greater the standard deviation, the greater the variability in the data. It is calculated by summing

the differences between each data point and the mean, squaring these differences, calculating the average of these squared values, and then taking the square root of this average. The standard deviation is useful for assessing how data is spread around the mean. The part below analyses the MATLAB code for the calculation of the error. In the code we rotate the vector A and B in the first part, then we create a vector X where we will put the two-vector representing the power received in each point and a vector vect_dif_27 that is at first zero and than we will put in it, the difference in measurements of each point at 27GHz. Same thing for the part concerning the 38GHz. Then the SD is calculated with a MATLAB function. To calculate the mean error, we simply added all the index of vect_diff_27 and divided them per 21. Same for 38GHz. We have then calculated the supplementary attenuation or penetration attenuation, which is the power that the floor slab has wasted during the measurement. The first image represents a scan of the slab which we made at a one floor distance and the second is the received power at 2 floor distance and it is done rotating the antenna in three positions (method explained in the third chapter).

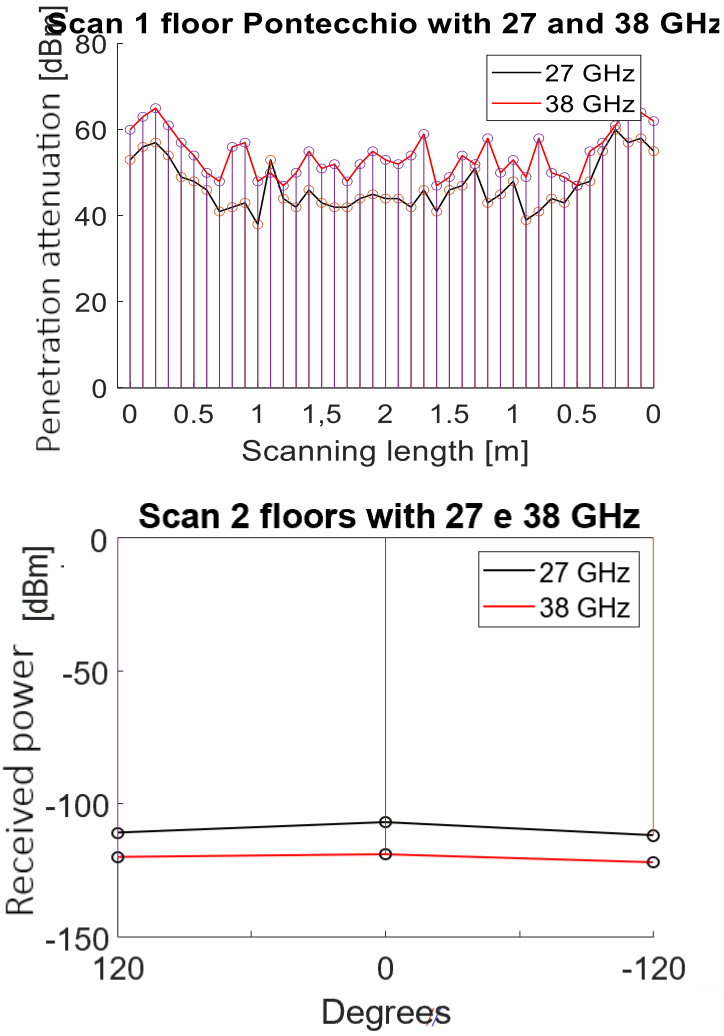

Figure 13 (high) penetration attenuation 1 floor Pontecchio
Figure 14 (low) penetration attenuation 2 floor Pontecchio

To calculate the supplementary attenuation, we built a function Friis27 (and Friis38) that returns the attenuation in LOS.

Parameters of this function are d distance, ptx which is the power transmitted, G1 and G2 which are the gain of the antennas and f the frequency.

In the initial tests, simulated values were observed to be several dBm higher than the measured values. To explain this difference, free-space measurements were conducted (in 2018) to calculate the actual power received by the antennas, we took then all the values elaborated by that time. In 2018 two directional antennas were placed at a distance of 15 meters and was established a radio link between them using the SAF kit equipment, the following average values were recorded following several tests, which varied by a few centimetres in positioning:

- 27GHz → Measured Pr =-49 dBm

- 38GHz → Measured Pr =-51 dBm

The measured values need to be compared with the theoretical values obtained by applying the Friis formula, which, in logarithmic form, becomes (4.2).

Substituting the theoretical values for the two frequencies under examination, the antenna gains from the datasheet, and the transmitted power values set through the signal generator, we obtain:

- 27GHz → Theoretical Pr =-42.6 dBm

- 38GHz → Theoretical Pr =-45.56 dBm

These values differ from the experimentally observed values, likely due to attenuation caused by connectors and cables. They might also include a difference between the actual antenna gain and the theoretical value presented in the antenna datasheet. To account for these losses, a correction factor was introduced, which differs for the two frequencies: 6.4 dBm for simulations conducted at 27 GHz and 5.44 dBm for simulations at 38 GHz. These factors were subtracted appropriately from all simulations to align the values correctly. This is why in the Friis function there's at the end a 6.4 and a 5.44 value. We then subtract from the power received the Friis LOS attenuation and we gained the supplementary attenuation [6].

4.2 Office area university building of 1930s

In DEI offices we made another scan as we did in Pontecchio.

This scan is the same length as the previous one, so 2 meters, and it is done back and forth. The distance of measure here is: 5.193 meters. It is plain a difference in the attenuation between the two frequencies, also if in some points there is no such difference, indeed there, the 38GHz frequency is above the 27GHz.

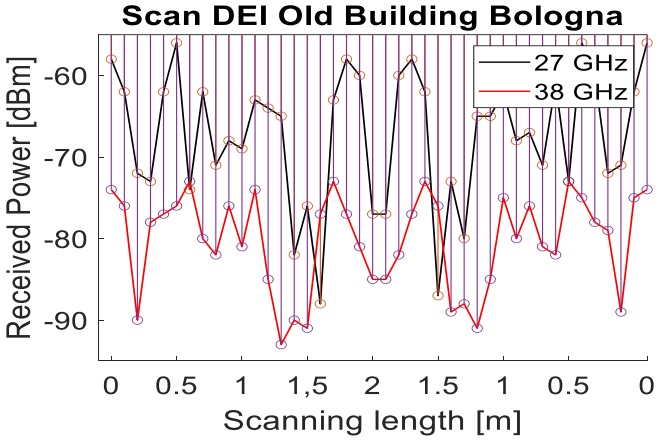

Figure 15 Scan DEI old building offices

This is a complex situation to analyse, in fact there are more than one reason why there is such rogue behaviour of the power received. One explanation is due to the materials which the slab is composed: they can have a different behaviour with different frequencies. Or another one is due to reflexions in the material because of the high frequency the signal can generate reflexion phenomena more complex that have an impact on the final result. So we can't say what has created that behaviour, in order to do so, we would have known what exactly there is in the floor slab and also its condition, the internal conditions of the slabs such as humidity can have had a great impact on the results reported. We made also in this case some calculus related to the mean error and the standard deviation.

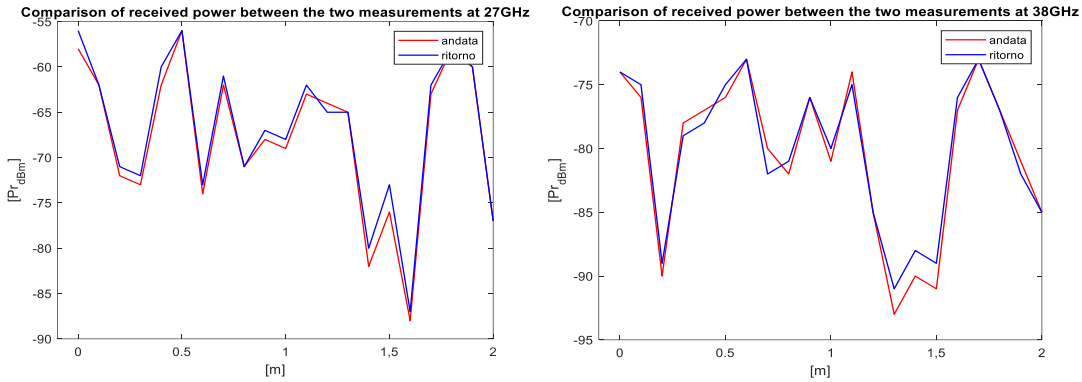

Figure 16 Comparison of received power between the two measurements at 27 GHz
Figure 17 Comparison of received power between the two measurements at 38 GHz

The calculus were dealt as before hitting a result of mean error at 27GHz and 38GHz respectively of: 0.904dB and 0.857dB. The result of standard deviation is: 8.210dB and 5.952dB. We than have calculated the penetration attenuation.

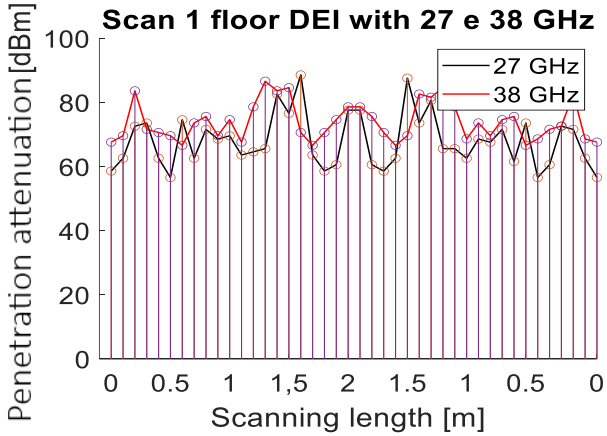

Figure 18 Penetration attenuation 1 floor DEI offices

4.3 Hall university building of 1930s

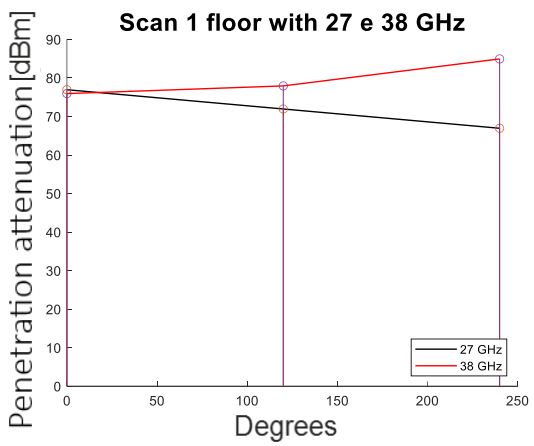

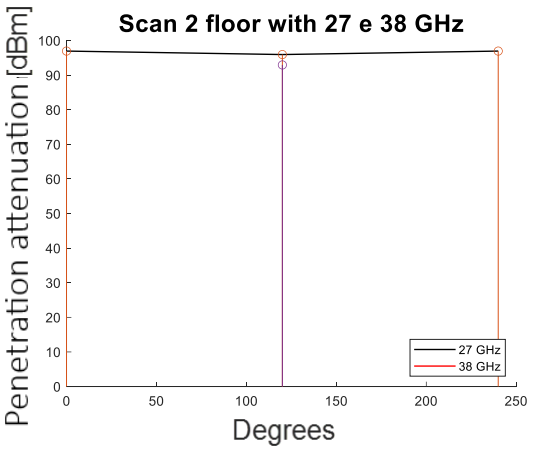

Figure 19 Penetration attenuation 1 floor DEI old building corridors
Figure 20 Penetration attenuation 2 floor DEI old building corridors

In Bologna corridors we have represented the same measurements that we made in Pontecchio at a two floor distance. We rotated the antennas. The distances of measure here are: 5.106 and 10 meters. Here is represented the supplementary attenuation from 1 floor distance and 2 floors distance. Since we haven't represented lot's of measure here we're not representing here the mean value and the standard deviation.

4.4 Office area university building of 1980s

In these two figures is represented the movement that we've done at DEI new building, moving the antenna to form a square. The side of square measures 2 meters, so each point is at two meters. The distance of measure here is of 3.5 meters. Due to the newest building process it has been difficult for us to take a lot of measures over the noise threshold, as we see in the two figures. The noise threshold is around-110dBm and here we have value in dBm that are just above that limit.

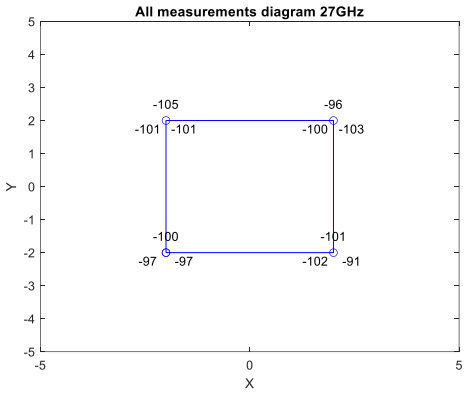

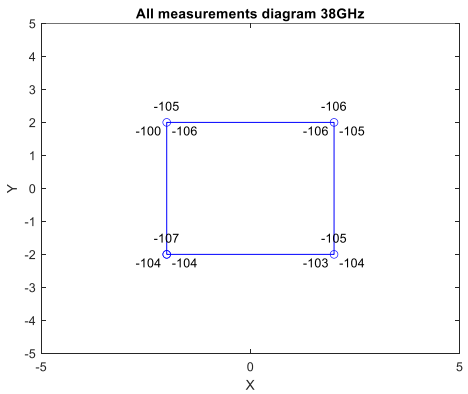

Figure 21 Rotational measurements in 4 points at DEI new building 27 GHz
Figure 22 Rotational measurements in 4 points at DEI new building 38 GHz

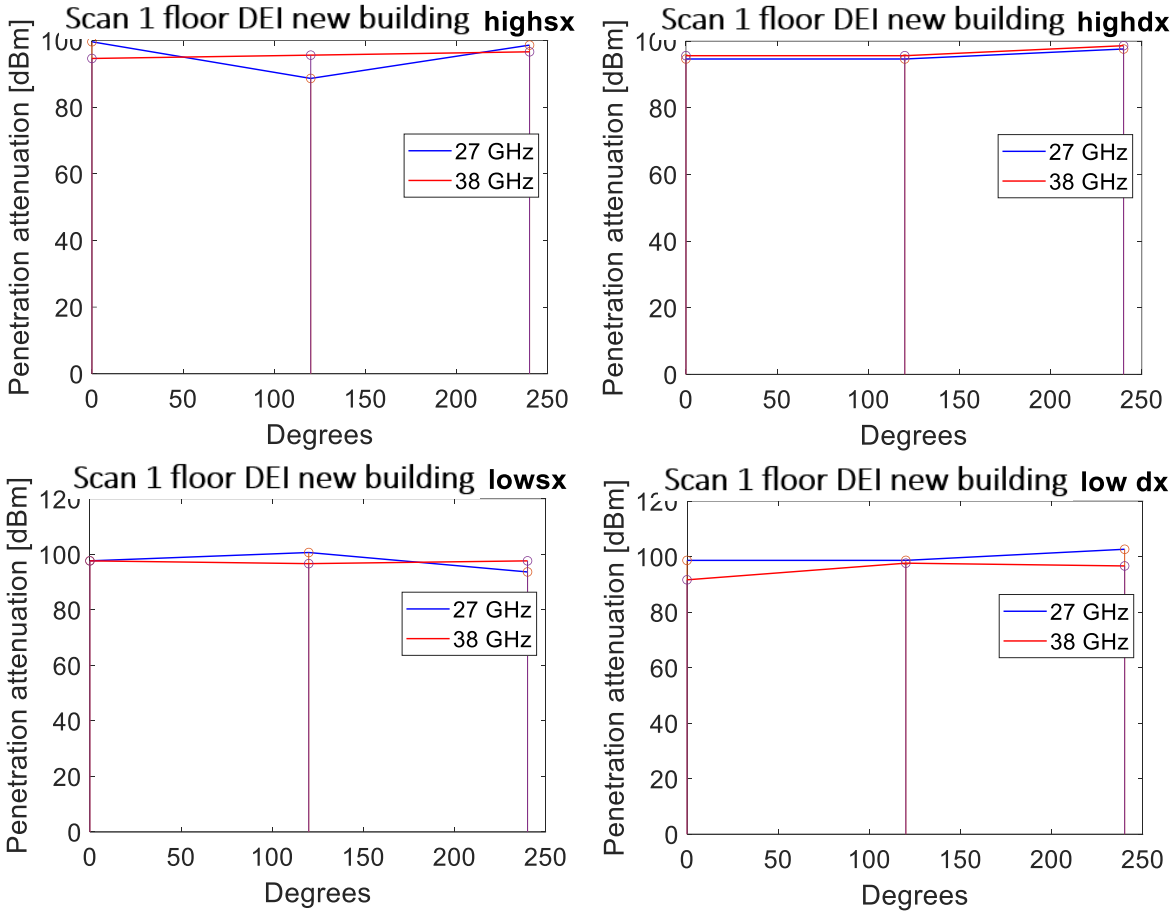

Figure 23 Scan 1 floor DEI new building (high left), Figure 24 Scan 1 floor DEI new building (high right), Figure 25 Scan 1 floor DEI new building (low left) and Figure 26 Scan 1 floor DEI new building (low right)

4.5 Modern university building of 2010

In the new headquarter of Cesena there wasn't any valid result above the noise threshold. This was due to a metallic net laid down on the floor that was added to other metal materials already existent in the floor. This was made maybe to reduce the acoustic reverb between the floors. Understanding the properties of metals is fundamental to grasp the behaviour of a wave incident upon them. The main characteristic that significantly sets metals apart from other materials is their conductivity. When we talk about conductive mediums, we consider the presence of free electric charges on their surface. In metals, these charges are electrons, and their movement generates an electric current. The current per unit area, denoted as $\mathcal{J}$, resulting from the application of the electric field $\boldsymbol{E}$, is related to the conductivity σ of the medium through the "constitutive law of the current field: $\mathcal{J} = \sigma\boldsymbol{E}$."

In metals, σ is non-zero and finite, whereas in a hypothetical ideal conductor, electrons simply follow variations in the electric field, and the only effect is re-emission without absorption and force

generation. When a wave impinges on a metal, it excites the free electrons, leading to the generation of heat and, consequently, the absorption of radiant energy. Thus, the absorption of radiant energy in a material depends on its conductivity, which is connected to the emergence of the Joule effect. The Joule effect is an irreversible phenomenon in which electromagnetic energy is transformed into heat, which is why an electromagnetic wave propagating in a conductor is gradually attenuated. In metals, thanks to their high conductivity, this effect is so significant that it renders them opaque. However, the strong absorption is accompanied by high reflectivity (or reflectance), which is why metallic surfaces serve as excellent mirrors.

This is why people use radars, which emit waves, to detect to detect airplanes and this is also the reason for which we haven't got any signal over the noise threshold.

CONCLUSION

For each floor slab we deducted generally, how the slab behaves when being crossed by a mm-wave. To do that we calculated the permittivity and the conductivity of the floor slab. In Cesena we have already discussed why we haven't received substantial values; in addition, we can say that the structure resembles in behaviour to an electric wave insulator cause of its high conductivity. The floor slabs, as we mentioned before, are difficult to manage because we don't know what there is inside. Usually there are some connectors used to bring water and electricity in the building. As time goes by the typical materials used for this purpose have changed, indeed we went from connectors in cast-iron, to cupper, to PVC. Not only the connectors have changed by time, also the way of construction for acoustic insulation, heat insulation, anti-seismic properties have developed. This has led to a wide possibility of materials used over time. We can approximate however, that in a certain period, the probability of having a floor slab built in a specific way is high.

For instance, nowadays all the connectors used are in PVC, if you go instead in a house built in the 20th century, you'll probably find copper. The pavement on which we walked is also formed by other materials, indeed it is composed in this manner:

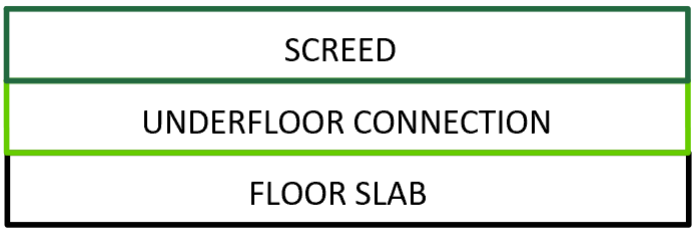

This is a basic representation of the structure of a pavement above the floor slab, this it is usually improved by adding some other parts such as:

vapour barrier, insulation panel and others.

Figure 27 Pavement basic structure

An ideal subfloor is one that provides good compression strength, effective insulation, and is lightweight to avoid overloading the floor structure. The underfloor connection part is filled then with different possible option, the same is with the screed [5].

All of this has not made our task easy. In Pontecchio, without considering all the connectors and other materials, we guessed that almost all the floor slab is made o wood, and calculating the theoretical supplementary attenuation the value verge on the one we measured with an acceptable difference, therefor sigma is 0.23 for 38 GHz and 0.16 for 27GHz and the epsilon$_r$ is 1.99. The other places we visited

are not as easy as Pontecchio because of their more complex internal structure. We can assume however a higher conductivity due to the usage of a bit of metal, concrete, brick, and other things as mentioned in chapter 3.

The conductivity is higher in DEI new classes than in DEI former building this is for most of the metal implied.
In all the measure that we took we must consider a static error that is due to our impossibility of knowing what's inside the slab. In fact, we could have measured a part containing things that have increased the attenuation or decreased. The probability of having a mean measure of a part with something inside that attenuates more and another one with something that attenuates less, is proportional to how many points on a line we have measured. This is why in Pontecchio and in DEI offices we performed a scan on a line. We can now form a table with the behaviour of the floor slabs.

The two values of DEI new classes and DEI former building, for what we said before are rough, but we wanted to give a glimpse on what are their approximate electrical properties.

Place	Distance(m)|slab width (cm)	Sigma 27GHz	Sigma 38GHz	Epsilonr	Rough materials	Period of construction	Mean supplementary attenuation 27GHz	Mean supplementary attenuation 38GHz
Pontecchio	4.241|22	0.160	0.230	1.99	Wood, others	17th Century	43.93	54.18
DEI old building	3.500|30	≈0.217	≈0.242	≈4.218	Concrete, brick, a bit of metal, others	≈1930	61.5	68.5
DEI new building	5.193|35	≈0.588	≈0.601	≈5.2	Concrete, brick, metal, others	≈1980	94.14	96.22
Cesena	3.500|30	Very high	Very high	≈1	Metal, concrete, others	≈2010	Undetectable	Undetectable

Table 5 Electrical properties and recap

In conclusion thanks to this table, we're able of making assumptions on the performance and the practical uses of the floor slab knowing the different period of construction and approximately the materials they're in and their proportion.

ACKNOWLEDGEMENTS

I would like to acknowledge the help provided by part of the Unibo DEI team: my primary supervisor Vittorio Degli Esposti, my second supervisor Enrico Maria Vitucci and Unibo's researcher Silvi Kodra whom offered deep insight into the study.

I would like to express my gratitude to my family and friends whom have supported me during my course of study.

BIBLIOGRAPHY

[1] S. Salous, V. Degli Esposti, F. Fuschini, D. Dupleich, R. Müller, R. S. Thomä, K. Haneda, J.M. Molina-Garcia-Pardo, J. Pascual-Garcia, D. P. Gaillot, M. Nekovee, S. Hur, "Millimeter-wave Propagation Characterization and Modelling Toward 5G Systems", IEEE Antennas and Propagation Magazine, vol. 58, no. 6, pp. 115-127, Dec. 2016

[2] T. S. Rappaport, R. Sun Shu, H. Z. Mayzus, Y. Azar, K. Wang, G. N. Wong, J. K. Schulz, M. Samimi, and F. Gutierrez, "Millimeter wave mobile communications for 5G cellular: It will work!" IEEE Access, vol. 1, 2013.

[3] Criticità strutturali dei solai in laterocemento e tecniche di rinforzo con nastri in composito | Articoli | Ingenio (ingenio-web.it)

[4] V. Degli-Esposti, "Propagazione e pianificazione nei sistemi d'area" 6_GTP_Ita2.pptx (sharepoint.com)

[5] Il sottofondo nei pavimenti | Fratelli Pellizzari

[6] M. Buccioli, V. Degli Esposti, E. Vitucci "Misure di Scattering a Onde Millimetriche in Ambiente Indoor" Tesi p.30-31